Lean NO$_x$ reduction on LNT-SCR dual-layer catalysts by H$_2$ and CO

Yi Liu, Yang Zheng, Michael P. Harold *, Dan Luss **

Department of Chemical & Biomolecular Engineering, University of Houston 77204-4004, TX, United States

ABSTRACT

Lean reduction of NO$_x$ (NO & NO$_2$) by H$_2$ and CO was conducted over monolithic catalysts consisting of a selective catalytic reduction (SCR) catalyst layer deposited on top of a lean NO$_x$ trap (LNT) catalyst. An increase in the CO/H$_2$ ratio decreased the cycle-averaged NO$_x$ conversion for the ceria-free LNT catalyst. CO poisoning was especially significant below 250 °C. The low-temperature NO$_x$ reduction was increased either by use of an LNT-SCR dual-layer catalyst or deposition of CeO$_2$ on the LNT catalyst. However, the ceria decreased the high-temperature reductive conversion of NO$_x$ due to promotion of the undesired NH$_3$ oxidation. Ceria zoning enhanced the monolith NO$_x$ conversion. Downstream loading of ceria led to the highest NO$_x$ reduction at both low- and high- temperatures due to the beneficial interaction of the ceria and H$_2$. The low-temperature NO$_x$ conversion of an aged dual-layer catalyst could be increased by a higher SCR catalyst loading. However, at high temperatures NO$_x$ reduction was independent of the SCR loading. The ratio of the lean to rich feed duration and the total cycle time were optimized to improve the NO$_x$ conversion in a temperature range from 150 to 400 °C. The highest cycle-averaged NO$_x$ conversion was obtained with a 30s:5s lean-rich cycle containing 1.25% total reductant for all CO/H$_2$ ratios for a lean feed containing 500 ppm NO and 5% O$_2$.

© 2012 Elsevier B.V. All rights reserved.

1. Introduction

The excess O$_2$ in diesel engine exhaust prevents NO$_x$ emission abatement by the well-established three-way converter (TWC). Two technologies exist for lean NO$_x$ reduction: selective catalytic reduction (SCR) and NO$_x$ storage and reduction (NSR). Urea–SCR, which uses urea-injection into the feed, is the leading technology for NO$_x$ emission reduction in heavy-duty diesel vehicles. NH$_3$ formed by thermal hydrolysis of the injected urea reacts with exhaust gases NO$_x$ and O$_2$ over Fe- or Cu-zeolite catalysts to produce N$_2$, H$_2$O and N$_2$O. Complex control strategies utilizing a NO$_x$ sensor manage the urea–SCR system [1,2]. The urea injection is plagued by problems, such as urea-fouling and NH$_3$ slip. The destruction of the slipped ammonia requires use of an expensive Pt-containing ammonia oxidation catalyst (AMOX) downstream of the SCR catalyst [3].

NSR technology is mainly applied for light-duty diesel and lean-burn gasoline vehicles, since the urea feed system is too cumbersome and expensive. NSR is carried out with rapid cycling between storage and reduction feeds. NO$_x$ and O$_2$ are stored on the lean NO$_x$ trap (LNT) catalyst, when the engine is running for the 30–60 s fuel-lean feed. Before significant NO$_x$ breaks through, the feed is shifted to a 5–20 s fuel-rich feed, which contains hydrocarbons, CO and H$_2$ formed by incomplete combustion of the fuel. The rich feed regenerates the stored nitrates and nitrites, forming N$_2$ and some NH$_3$. Periodic operation at rather high frequency demands the LNT catalyst to perform rapid NO$_x$ storage and reduction. A high loading of expensive precious group metals (PGM), i.e., Pt and Rh, is typically used to promote the fast kinetics that is required [4,5] and to extend the LNT life. The LNT catalyst contains barium and/or potassium oxides as NO$_x$ storage components, ceria or ceria-zirconium as promoters and surface stabilizers, and γ-Al$_2$O$_3$ as a high surface area support. The NSR technology is only applied to light-duty diesel and lean-burn gasoline vehicles, where the exhaust flow rates are low and hence small NO$_x$ traps can be used.

An economic alternative for lean NO$_x$ abatement is a combination of NSR and SCR catalysts, called LNT/SCR (or sometimes NSR/SCR) catalyst. The joint application of LNT and SCR catalysts can lead to a higher NO$_x$ conversion and N$_2$ selectivity than by using only the LNT catalyst [6–10]. Potential catalyst architectures are sequential multi-brick, multi-layer, and mixed catalysts. A detailed review was presented in [11]. In these systems, the

* Corresponding author. Tel.: +1 7137434307; fax: +1 7137434323.
** Corresponding author.
E-mail addresses: mharold@uh.edu (M.P. Harold), dluss@uh.edu (D. Luss).

LNT captures a large fraction of the NO_x during the fuel-lean mode, and the stored NO_x is reduced to N_2 and some NH_3 during the fuel-rich mode. The adjacent or downstream SCR catalyst stores the NH_3 product on its Brønsted and Lewis acid sites during the fuel-rich mode, and the captured NH_3 reduces NO_x during the subsequent fuel-lean feed. Thus, the SCR catalyst utilizes the NH_3 generated by the LNT for additional NO_x reduction, thereby replacing the expensive urea-injection system by an in situ NH_3 generation system. In a dual-layer catalyst system the LNT and SCR are in intimate contact but the operating principle remains essentially the same. When the SCR layer is coated on top of the LNT layer, NO_x that diffuses into the SCR catalyst during the lean fuel mode may either react with NH_3 or diffuse to the underlying LNT layer where it is stored, and then may be reduced to N_2 or NH_3 during the next fuel-rich mode. Thus, since only a fraction of the fed NO_x has to be reduced on the LNT, a fraction of the expensive LNT catalyst may be replaced by the less expensive SCR catalyst.

NH_3 is the key chemical link between the LNT and SCR catalysts. Thus it is important to use reductants that promote NH_3 generation by the LNT catalyst. LNT regeneration by H_2 has been extensively studied [12–15]. However, during rich operation typical vehicle exhaust contains a complex mixture of CO, H_2 and hydrocarbons. The CO/H_2 ratio in lean-burn gasoline exhaust is about 3 [16]. For diesel vehicles the H_2 concentration is lower while the hydrocarbon fraction is higher and can contain a wide range of hydrocarbons. The upstream diesel oxidation catalyst (DOC) reduces the concentrations of these species, but during rich operation these species may reach the LNT. A desired catalyst should also be a stable NH_3 generator and insensitive to whether the feed contains H_2, CO, and/or hydrocarbons. The concentrations of CO and H_2 depend on the air-to-fuel ratio during the regeneration. For example, an air-to-fuel ratio of 9.0 may favor H_2 generation, while an air-to-fuel ratio between 12.0 and 13.0 may favor CO generation [17]. Hence, the LNT catalyst may be exposed to varying CO/H_2 ratios during the regeneration. Studies of LNT regeneration using CO as the reductant have elucidated the reaction pathways and dynamic performance [18–28]. The key findings are: that H_2 out-performs CO as a LNT reductant mainly due to the lack of the self-inhibition encountered with CO that binds to the Pt catalyst; Several reaction pathways may lead to NO_x reduction by CO. Including formation of an intermediate isocyanate (NCO_{ad}) followed by reaction with additional stored NO_x and H_2O (hydrolysis) to produce a mixture of N_2O, NH_3 and N_2 [18–22,28].

The direct reduction of NO_x by CO in the absence of H_2O leads to a mixture of N_2O and N_2 with selectivities dictated primarily by the effective NO_x/CO ratio. This may involve the formation of the surface isocyanates (NCO_{ad}). Forzatti et al. [18] proposed a Pt-catalyzed reaction pathway including the reduction of nitrates (NO_3^-) by CO to nitrites (NO_2^-) and sequential reduction to isocyanate/cyanate species, which react with additional nitrites to N_2. Residual isocyanate/cyanate species are oxidized by O_2 and NO_x in the lean feed to N_2 and surface nitrites. Castoldi et al. [19] found that the isocyanate reaction pathway was the main route for NO_x reduction by CO over a $Pt/K/Al_2O_3$ LNT catalyst. The, reaction between NCO_{ad} and nitrates was faster over $Pt/K/Al_2O_3$ than over $Pt/BaO/Al_2O_3$. DiGiulio et al. [20] investigated the regeneration of Pt- and $Rh-BaO/Al_2O_3$ LNT catalyst with CO and propylene. Surface isocyanate species were identified as key intermediates by in situ FTIR spectroscopy. Reactions of NCO_{ad} with NO_x and O_2 forming N_2 were catalyzed by the precious metal catalyst, while NH_3 formation from the NCO_{ad} hydrolysis was not.

Studies with different reductants found H_2 to be a more effective reductant for surface nitrate regeneration than CO or hydrocarbon, especially at low temperatures. Theis et al. [21] found that

at low temperatures H_2 was a more effective reductant of LNT stored NO_x than CO or C_3H_6. A possible pathway for CO reduction in the presence of H_2O is H_2 formation via water-gas-shift reaction ($CO + H_2O \leftrightarrow H_2 + CO_2$). Szailer et al. [22] used in-situ FTIR and time-resolved XRD to compare the reduction by H_2 and CO over a $Pt/BaO/Al_2O_3$ were effectively reduced by H_2 at low temperatures. When CO was the reductant, NCO_{ad} species that accumulated on the metal oxides surface reacted with NO_x at high temperatures. In the presence of H_2O, the hydrolysis of NCO_{ad} species formed NH_3 and CO_2. James et al. [23] found that CO facilitated the decomposition of barium nitrates but could not reduce the released NO_x to N_2 due to the strong affinity of CO and Pt. H_2 assisted both the nitrate decomposition and NO_x reduction. Poulston and Rajaram [24] found that H_2 was a better reductant than CO for regeneration of aged LNT catalyst. Li et al. [25] found that H_2 was the a more effective reductant than HC and CO on a $Pt/Rh/BaO/Al_2O_3$ LNT catalyst below 200 °C. Scholz et al. [26] found that H_2, CO and C_2H_4 had comparable NO_x reduction efficiencies over a $Pt/BaO/Al_2O_3$ catalyst at 300 °C. The addition of H_2O prevented CO and C_2H_4 poisoning of Pt. Jozsa et al. [27] reported that. H_2 was a more effective reducing agent of LNT catalysts than CO, C_3H_6, especially at low temperatures. Dasari et al. recently [28] compared the steady-state anaerobic reduction of NO with CO in the presence and absence of water with the reduction by H_2. The enhanced NO reduction by CO in the presence of H_2O may be explained by formation of H_2 by the water gas shift reaction. However, in more recent work the behavior changes under transient conditions when the isocyanate pathway emerged as an important one for NO_x reduction.

Several researchers studied the regeneration of LNT-SCR dual-bed and mixture catalysts with CO. Corbos et al. [29] used CO to reduce the stored NO_x on $Pt-Rh/Ba/Al_2O_3$ and Cu/ZSM-5 mixture catalyst. Cu/ZSM-5 facilitated the reactions between CO and NO_x to form the surface NCO species. The hydrolysis of NCO_{ad} species generated NH_3 and sequential NO_x reduction over the SCR catalyst. The highest NO_x conversion from the LNT-SCR mixture catalyst occurred when both H_2 and CO were used as reductants. Researchers from the University of Kentucky and Ford Motor Co. [30] investigated the NO_x reduction on LNT-SCR multi-brick catalyst by H_2, CO and C_3H_6. Some NO_x was reduced by the adsorbed hydrocarbons over the Cu-zeolite, in addition to the conventional NH_3-SCR pathway.

We extend here our previous report [11] of lean NO_x reduction with H_2 and CO over several synthesized dual-layer catalysts. The goal is to determine the impact of reductant composition, catalyst composition profile, reactor configuration, and lean-rich switching policy on cycle-averaged NO_x conversion and product selectivity. The results suggest ways to reduce the loading of the expensive PGM while maintaining a high NO_x conversion.

2. Experimental

2.1. Catalyst preparation

Monolithic LNT bricks were supplied by BASF Catalysts (Iselin, New Jersey). Each channel in the cordierite substrate ($\sim$62 channels/cm^2) was coated with a washcoat layer with a thickness of 60–80 μm. The LNT washcoat load was rather high of 4.6 g/in^3. Cylindrical cores ($D = 2.5$ cm, $L = 7.6$ cm) were drilled out of the monolithic brick from which small monolithic pieces were prepared with a specific shape (28 channels; $D = 0.8$ cm, $L = 2.0$ cm). Three LNT catalysts with the same PGM and barium oxide loading were used in our study. Their compositions are reported in Table 1. Their ceria loading varied from 0 wt% (LNT1) to 34 wt% (LNT3). Aged LNT catalysts were prepared by calcining the monolithic pieces at 600 °C in dry air for 100 h. Cu/ZSM-5 powder was

Table 1
The LNT catalyst compositions.

	Pt/Rh (g/ft^3)	BaO (wt%)	CeO_2 (wt%)
LNT1	90	14	0
LNT2	90	14	17
LNT3	90	14	34

synthesized by the wet-ion exchange method reported by Liu et al. [11]. The dual-layer catalyst was prepared by dip-coating a slurry containing a milled Cu/ZSM-5 onto the LNT monolithic piece. A desired SCR loading was obtained by repeated dip-coating [31]. Unless specifically stated, the SCR loading was of $0.9 \, g/in^3$ and the total washcoat loading was approximately $5.5 \, g/in^3$. In some experiments, a higher SCR loading of $2.0 \, g/in^3$ was used, giving a total washcoat loading of $6.6 \, g/in^3$. The smallest (side wall) washcoat thicknesses of the $5.5 \, g/in^3$ and $6.6 \, g/in^3$ samples were approximately 120 and $170 \, \mu m$, respectively, as measured by SEM.

2.2. Reactor tests

The bench-scale reactor set-up was described in previous studies [32–35]. A series of mass flow controllers (MKS Inc.) controlled the gas flow rates, and a syringe pump (ISCO Model 500D) fed the water. The feed to the reactor was controlled by a switching valve positioned upstream of the reactor. The monolith was wrapped by Fiberfrax® ceramic paper and installed in a quartz tube reactor (1.2 cm diameter, 40.6 cm length; Technical Glass Products), inserted in a tube furnace (Mellen M300) for temperature control. The temperature inside the reactor was measured by two 0.5 mm type-K stainless steel sheathed thermocouples (Omega Engineering Inc.); one placed 0.5 cm in front of the monolith to measure the feed temperature and the second placed in the middle of the center channel of the monolith to measure the catalyst temperature. The gaseous effluent from the reactor was measured sequentially by a FTIR (Thermo Nicolet Nexus 470) and a quadrupole mass spectroscopy (QMS; Cirrus LM99, MKS Inc.). The FTIR monitored the concentrations of the NO, NO_2, N_2O, NH_3, CO, CO_2 and H_2O, while the QMS monitored the concentrations of H_2 and O_2. In the presence of CO, the overlap of the $m/e = 28$ in the QMS ruled out N_2 measurement. Thus, the steady-state N_2 formed was determined by closing an overall nitrogen balance. The FTIR and QMS were calibrated daily.

The fuel-lean and -rich cycles were generated by periodic shifts between the lean and rich feeds. The Ar carrier gas contained 2.5% H_2O and 2.0% CO_2. The lean feed contained 500 ppm NO and 5% O_2 in the carrier gas mixture. It was fed between 6s to 60s. The rich feed contained 2.5% reductant but no NO and O_2 in the same carrier gas. Three reductant feeds were used: 2.5% H_2, 2.0% H_2/0.5% CO and 1.5% H_2/1.0% CO. The corresponding CO/H_2 ratios were 0, 0.25 and 0.67, respectively. The duration of the rich feed varied from 1 to 20 s. The cycle average H_2/NO feed ratio was 1.04 times the stoichiometric ratio needed for NH_3 formation by the reaction:

$$16H_2 + 4NO + 3O_2 \leftrightarrow 4NH_3 + 10H_2O \tag{R1}$$

It took approximately 10 min to reach a periodic state. The feed temperature was increased from 150 to 400 °C in steps of 50 °C. At least 25 cycles were run at each temperature. The cycle-averaged NO_x conversion and product selectivity were obtained by averaging the last ten lean-rich cycles. The NO_x conversion, the NH_3 and NO_2 selectivity (S_A), and the N_2O selectivity (S_B) were calculated by
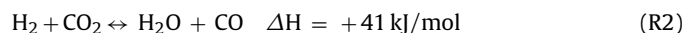
$$X_{NO_x} = 1 - \frac{\int_0^{\tau_s} [F_{NO}(t) + F_{NO_2}(t)]dt}{\int_0^{\tau_l} F_{NO}^i(t)dt} \tag{1}$$

$$S_A = \frac{\int_0^{\tau_s} F_A(t)dt}{\int_{\sim 0}^{\tau_l} F_{NO}^i(t)dt - \int_0^{\tau_s} F_{NO}(t)dt} \tag{2}$$

$$S_B = \frac{\int_0^{\tau_s} 2 * F_B(t)dt}{\int_0^{\tau_l} F_{NO}^i(t)dt - \int_0^{\tau_s} F_{NO}(t)dt} \tag{3}$$

Here τ_l and τ_s are the duration of lean phase feed and the lean-rich total cycle (s). F_{NO}^i and $F_{NO}(t)$ are the NO feed $F_{NO}(t)$ and effluent molar flow rates (mol/s). $F_A(t)$ is the effluent molar flow rates of either NH_3 or NO_2 and $F_B(t)$ the effluent molar flow rate of N_2O (mol/s).

A few stationary experiments were conducted over the LNT catalysts to assess the activity of the reverse water-gas-shift reaction (rWGS); i.e.

$$H_2 + CO_2 \leftrightarrow H_2O + CO \quad \Delta H = +41 \, kJ/mol \tag{R2}$$

The total flow rate was 1000 sccm (GHSV = 60,000 h^{-1}, based on total monolith volume and standard conditions). It contained 500 ppm CO and 2.5% H_2O in Ar.

3. Results and discussion

3.1. Effect of CO/H_2 ratio on NO_x reduction on LNT catalysts

Experiments were conducted to compare the NO_x conversion and product distribution of the three LNT catalysts. Fig. 1 shows the NO_x conversion for the ceria-free LNT1 catalyst exposed to a 60s lean/5s rich cycle over a range of feed temperatures. The rich feed contained 2.5% reductant in a carrier gas mixture of CO_2, H_2O and Ar. The solid line describes the NO_x conversion as a function of feed temperature using 2.5% H_2 as the sole reductant. The dashed and dotted lines represent the NO_x reduction by CO/H_2 mixtures with ratios of 0.25 and 0.67, respectively. The NO_x conversion using 2.5% H_2 feed had a local minimum at 200 °C and a local maximum at 350 °C. The NO_x conversion decrease above 350 °C is likely due to the decreasing stability and an increasing decomposition rate of stored NO_x [15]. The NO_x conversion at 200 °C is close to that obtained for a rich feed having 0.5% CO in 2% H_2. The conversion decrease between 150 and 200 °C could be caused in part by the reverse water gas shift reaction, $CO_2 + H_2 \leftrightarrow CO + H_2O$ [15,35] which we discuss in more detail later. The NO_x conversions of CO-containing feeds were lower than those of feeds containing only H_2 at temperatures below 250 °C. For example, at 150 °C the NO_x conversion of a CO-free feed was 54% and 15% for a feed with $CO/H_2 = 0.67$. The differences between the NO_x conversions for the three different feeds diminished at temperatures exceeding 200 °C. The NO_x reduction of mixtures of H_2 and CO was slightly higher than that of a feed of pure H_2 at temperatures exceeding 350 °C.
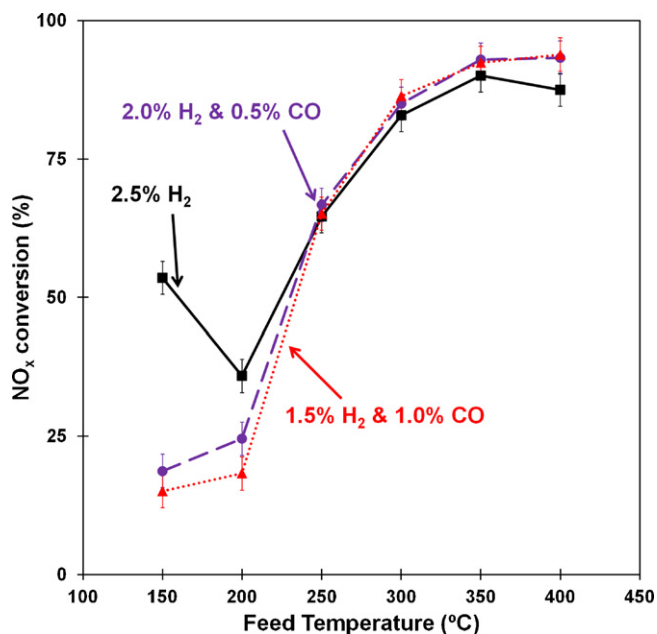
Fig. 1. Comparison of NO_x conversion by LNT1 catalyst using a mixture containing 2.5% reductants with different CO/H_2 ratios. The carrier gas contained 2.5% H_2O and 2.0% CO_2 in Ar.

The presence of CO greatly diminishes the low-temperature NO_x conversion. This is evident from Fig. 2a and b that show the transient effluent composition from the LNT1 catalyst during the 5 s rich phase and 5 s of the subsequent lean phase during two typical lean (60s)–rich (5s) cycles, using 2.5% H_2 to regenerate the catalyst. At both 150 °C and 200 °C, N_2O immediately formed during the rich phase, followed by the formation of NH_3. CO appeared after NH_3 at 200 °C, while no CO was detected at 150 °C. The appearance of NH_3 is a product of deep reduction. At a temperature of 200 °C and higher, H_2 reacts with CO_2 fed in the carrier gas to generate CO via
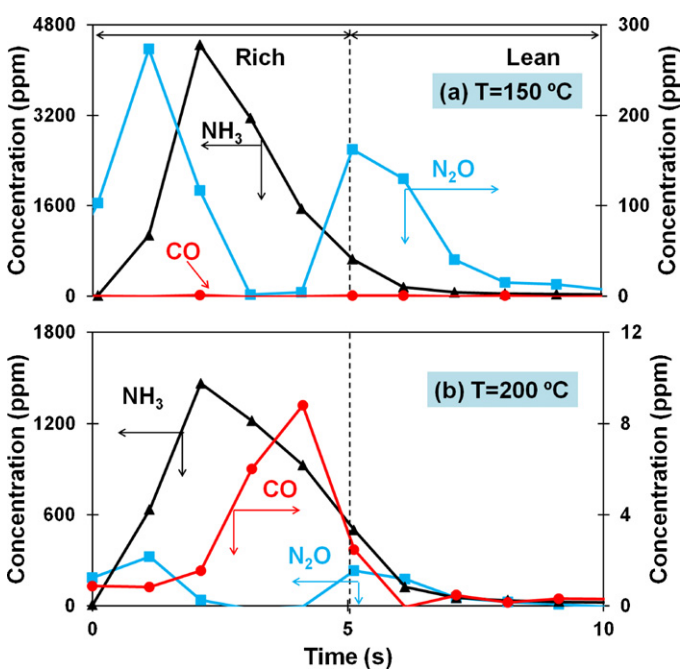

Fig. 2. The effluent concentrations during the 5 s of rich feed and subsequent 5 s of lean feed using LNT1 at (a) 150 °C and (b) 200 °C. The reductant was 2.5% H_2 and the cyclic feed was of 60 s lean and 5 s rich. The carrier gas contained 2.5% H_2O and 2.0% CO_2 in Ar.

the reverse water-gas-shift reaction. The CO breakthrough at 200 °C using pure H_2 as the reductant suggests that a fraction of the active PGM sites are occupied by CO. This may decrease the rates of NO_x storage and reduction. The absence of CO at 150 °C infers that the extent of reaction between H_2 and CO_2 is negligible, and therefore more free PGM sites are available for the NO_x reduction to occur than at 200 °C.

The CO inhibition is more significant when CO is added to the feed. This is evident from the much lower NO_x conversion using CO mixtures to conduct the regeneration at 200 °C. The CO inhibition decreases at higher temperatures, probably due to an increased rate of CO desorption; the binding energy of CO on Pt is between 80 and 120 kJ/mol. The data also show that the presence of CO in the reductant mixture increases the NO_x reduction above 250 °C. According to James et al. [23], CO facilitates the decomposition of barium nitrates both on the surface and in the bulk. Thus, a more complete regeneration at high temperatures can be achieved using both H_2 and CO compared to pure H_2. The higher utilization of NO_x storage sites on the surface and in the bulk increases the NO_x conversion above that attained with pure H_2 reductant. Corbos et al. [29,36] also reported that using a H_2 and CO mixture led to the highest NO_x conversion from a LNT-SCR mixture catalyst.

These trends suggest that the presence of CO in the reductant mixture has a significant impact on the regeneration chemistry. When pure H_2 is used as the sole reductant, CO is produced above 200 °C according to Fig. 2. The generated CO binds to the PGM and inhibits the deep reduction of the stored NO_x [17,22,35]. As a result, the NH_3 selectivity has a local minimum at 200 °C. The diminution of NH_3 generation in the lower temperature range is more pronounced when CO is present in the reductant mixture. The lower the CO/H_2 ratio the higher is the NH_3 selectivity. A temperature increase leads to an increase in the rate of CO desorption and of the water-gas-shift (WGS) reaction. This trend increases the availability of PGM sites for catalyst regeneration and of H_2 for NH_3 generation. Thus, NH_3 selectivity from NO_x reduction with H_2 and CO increases with temperature up to 250 °C. For all the reductant mixtures increasing the temperature decreases the NH_3 selectivity due to sequential reaction with stored NO_x downstream of its generation [11,37,38]. The N_2 selectivity increases at the expense of the NH_3 selectivity decrease for all reductant mixture compositions.

The assertions that the forward and reverse WGS reactions have an impact can be checked by evaluating the steady-state activity of the Pt/BaO catalyst. First, we suggest that mitigation of the inhibition caused by CO chemisorption is due in part to the forward water-gas-shift chemistry which converts CO to CO_2. Fig. 3a shows that the steady-state WGS conversion rises steeply at 250–200 °C for the LNT1 catalyst. The conversion is close to 100% at 350 °C. The addition of ceria to the catalyst (LNT3) results in a higher conversion, as we discuss later. Second, based on earlier discussion, the formation of CO via the reverse water gas shift reaction for a feed containing H_2 and CO_2 (no CO) may contribute to the decrease in the NO_x conversion between 150 and 200 °C; i.e. local minimum at 200 °C (Fig. 2). However, the rather low extent of the reverse WGS reaction at 200 °C (Fig. 3b) suggests it is not the main cause for the local minimum. We are investigating this issue in more detail and will report the results elsewhere.

The CO/H_2 ratio affects both the NO_x reduction and the product distribution. Fig. 4 compares the N_2 and NH_3 selectivities using LNT1 catalyst with reductant mixtures containing different CO/H_2 ratios but fixed total reductant concentration (2.5%). When pure H_2 was used as the reducing agent, the NH_3 selectivity decreased with temperature while the N_2 selectivity increased, except at 200 °C where a local minimum in the NH_3 selectivity (39%) was obtained. In contrast, for NO_x reduction by the H_2 and CO mixture, the NH_3 selectivity increased with temperature below 250 °C and then decreased. The temperature dependence of N_2 selectivity was
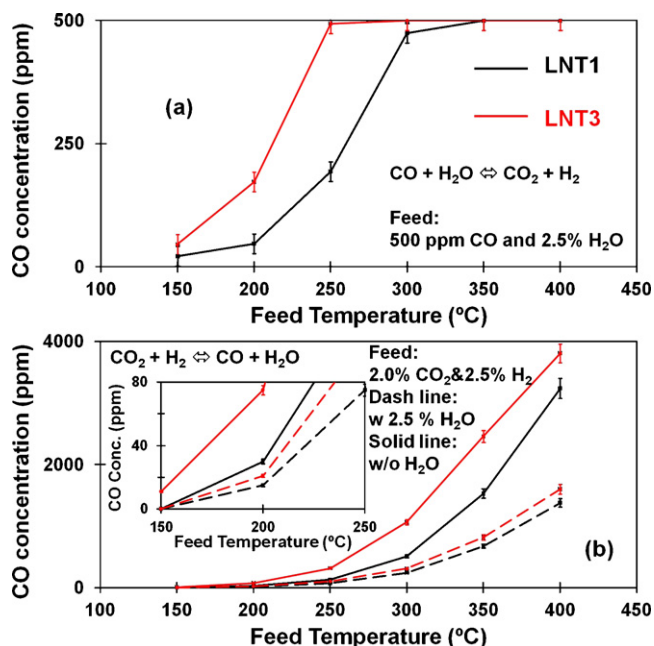
Fig. 3. (a) CO_2 formation by the water-gas-shift reaction and (b) CO formation by the reverse water-gas-shift reaction conducted over LNT1 and LNT3.

in general the inverse of the NH_3 selectivity since these two were the primary N-containing products at higher temperature. The NO_x reduction with pure H_2 led to a higher NH_3 selectivity than using mixtures of H_2 and CO over the entire temperature range.

3.2. LNT/SCR dual-layer catalysts for CO/H_2 reductant mixtures

The rather high NH_3 selectivities (>50%) obtained with the LNT1 catalyst suggests that a dual layer catalyst will enhance the selectivity to N_2. We have previously shown that this is the case by using H_2 as the sole reductant in the absence and presence of CO_2 and H_2O [11,35]. Fig. 5 compares the NO_x conversions from LNT1 and CuZ-LNT1 catalysts using reductant mixtures with the same three CO/H_2
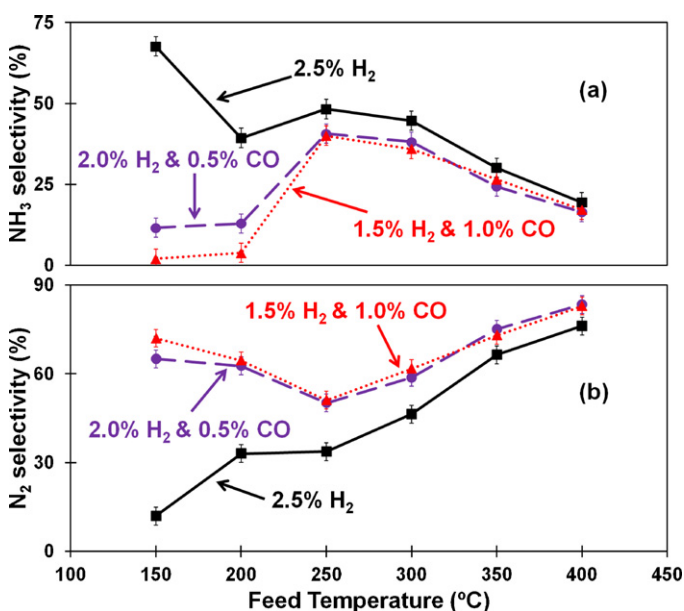

Fig. 4. Comparison of (a) NH_3 and (b) N_2 selectivities. Catalyst was LNT1. Feed contained 2.5% reductants with different CO/H_2 ratios. The carrier gas contained 2.5% H_2O and 2.0% CO_2 in Ar.
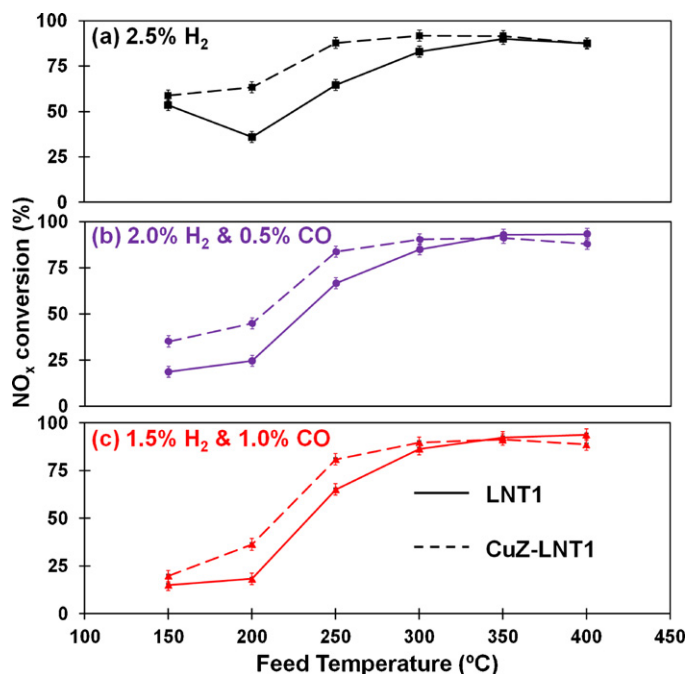

Fig. 5. Comparison of the NO_x conversion using mixtures with 2.5% reductants with different CO/H_2 ratios conducted over LNT1 and CuZ-LNT1. The carrier gas contained 2.5% H_2O and 2.0% CO_2 in Ar.

ratios as earlier. The solid lines describe the LNT1 catalyst performance, and the dashed lines those of the corresponding dual-layer catalyst. The dual-layer catalyst had a higher low-temperature NO_x conversion than the LNT1 catalyst for all temperatures except for 400 °C. The increase in NO_x conversion from the dual-layer catalyst decreased with an increase of the CO/H_2 ratio. At 200 °C, the NO_x conversion increase was 27%, 21% and 18% for mixtures with a CO/H_2 ratio of 0, 0.25 and 0.67, respectively.

The addition of the Cu/ZSM-5 SCR catalyst layer contributes selective NO_x reduction activity to the standard SCR reaction between NH_3, NO and O_2. When the dual-layer catalyst is used, NH_3 produced in the underlying LNT layer during the rich phase is captured by the SCR top-layer due to the strong binding of NH_3 to the Cu/ZSM-5, decreasing the NH_3 slip [11]. The NH_3 stored in the SCR catalyst reduces the NO_x fed during the lean phase, generating N_2 with high selectivity. Fig. 6 shows the enhancement in the N_2 selectivity with the deposition of the CuZ layer on top of the LNT1 layer. The large increase in the N_2 selectivity shows the effective SCR utilization of the stored NH_3 for NO_x reduction chemistry. An increase in the CO/H_2 ratio decreases the extent of NO_x reduction since CO decreases the NH_3 selectivity, as shown in Fig. 4. The LNT1 reduction with CO and H_2 mixture can be improved by depositing a SCR-layer on top of the LNT layer.

3.3. Effect of Ceria in the LNT Layer

Optimizing the catalyst design variables, such as the ceria loading in the LNT layer can minimize the impact of the CO/H_2 ratio on the NO_x conversion, especially at low temperatures. Ceria provides several functions. First, it enhances the activity of Pt. Phatak et al. [39] reported that the turnover frequency of ceria-supported Pt is 30 times higher than that of alumina-supported Pt. Ceria also provides additional NO_x storage sites, especially below 250 °C [40] and it mitigates CO inhibition by either enhancing the oxidation of CO or when H_2O is present, enhancing the water-gas-shift reaction. By adding ceria, the Pt-catalyzed CO oxidation reaction order changes from −1 to 0 [41,42]. We showed that CO oxidation can be
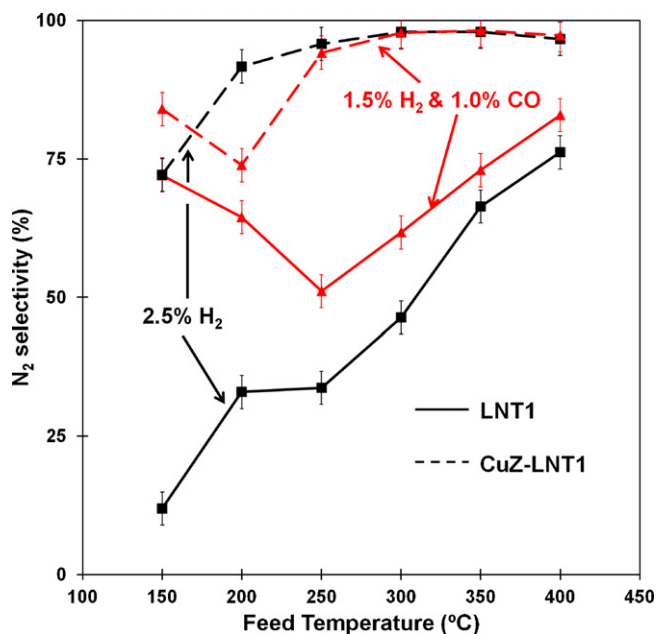
Fig. 6. Impact of CO/H_2 ratio on the N_2 selectivity over LNT1 and CuZ-LNT1.

carried out even at $150\,°C$ over a Pt/CeO_2 catalyst [16]. Other benefits from the ceria addition include the resistance toward hydrothermal aging through the stabilization of Pt crystallites and the mitigation of SO_x poisoning. For these reasons, a LNT catalyst containing ceria was used in the study of the dual-layer catalyst.

The temperature dependence of NO_x conversion for the ceria-free LNT1 and ceria-rich LNT3 catalysts is shown in Fig. 7 using mixtures with different CO/H_2 ratios. The NO_x conversion by the LNT3 catalyst was up to 35% (absolute) higher than that by the LNT1 catalyst. For example, the NO_x conversion by LNT3 was 71% at $200\,°C$, while the NO_x conversion by LNT1 was 36% using 2.5% H_2. Increasing the CO/H_2 ratio decreased the NO_x conversion using
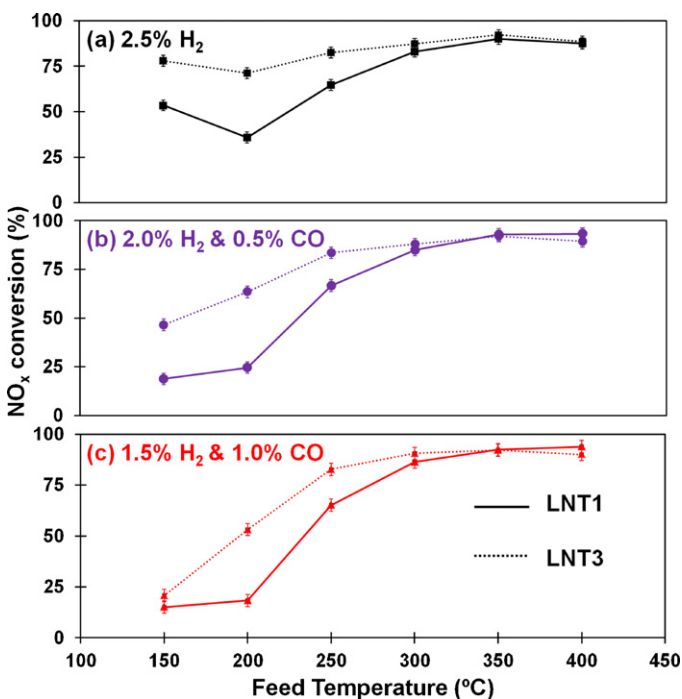

Fig. 7. impact of CO/H_2 ratio on NO_x conversion over LNT1 and LNT3.
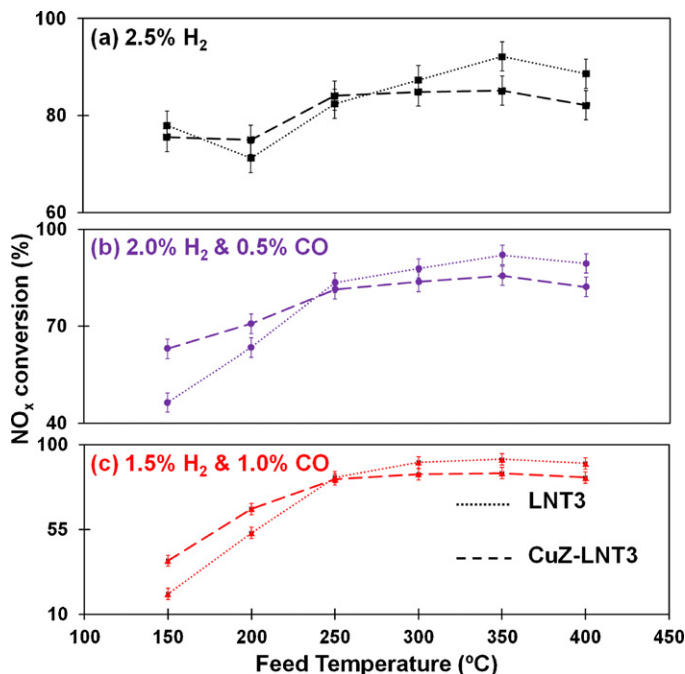

Fig. 8. NO_x conversion by LNT3 and CuZ-LNT3 using three different 2.5% CO/H_2 reductant mixtures The carrier gas contained 2.5% H_2O and 2.0% CO_2 in Ar.

either the LNT1 or LNT3 catalyst. The increase in the NO_x conversion achieved with the addition of ceria (LNT1 to LNT3) was unaffected by the CO/H_2 ratio, except at $150\,°C$.

The effect of ceria on the WGS activity of the Pt catalyst was made evident in steady-state experiments (Fig. 3). The addition of ceria has an important effect in mitigating the effect of CO but also in producing CO from CO_2 and H_2. The light-off temperature, defined as the temperature at 50% CO conversion ($T_{50\%}$), was approximately $50\,°C$ lower for LNT3 (ceria rich) than for LNT1 (ceria free). Thus, the effective CO removal and subsequent H_2 generation increases the low-temperature performance of LNT3. Fig. 3b shows the reverse water-gas-shift reaction over LNT1 and LNT3 catalysts generated CO from a mixture of H_2 (2.5%) and CO_2 (2%) with and without water even at $200\,°C$. Fig. 3a and b shows that the extent of the reverse WGS reaction is smaller than that of WGS reaction. For example, at $200\,°C$ the CO conversion over LNT3 was 35% while the CO_2 conversion was only 0.11%. As the water gas shift reaction is exothermic thermodynamics favors the forward reaction. Thus, ceria addition primarily enhances the CO conversion to H_2 and promotes the low-temperature performance of the LNT catalyst. This conclusion agrees with the findings of Honda researchers [37,38]. In a narrow temperature window the reverse water gas shift reaction inhibits the NO_x conversion.

Fig. 8 compares the NO_x conversions by the LNT3 catalyst and the corresponding dual-layer catalyst using different reductant compositions. (Note: A comparison of the CuZ/LNT1 and CuZ/LNT3 catalysts is made later.) When 2.5% H_2 was used as the reductant, the dual-layer catalyst resulted in a slightly higher NO_x conversion than the LNT3 catalyst at 200 and $250\,°C$, but a 5–7% lower NO_x conversion above $250\,°C$. For higher CO/H_2 ratios, the enhanced conversion by the SCR addition was more significant at low temperatures. However, the dual-layer catalyst NO_x conversion was still lower than that of LNT3 above $250\,°C$.

The lower high-temperature NO_x conversion of the dual-layer catalyst is likely due to the addition of ceria. As we showed earlier [11,35], the oxidation of stored NH_3 is increased in ceria-containing LNTs during the lean phase. That is, the NH_3 stored in the top SCR layer, which desorbs at high temperatures, can be oxidized to NO_x
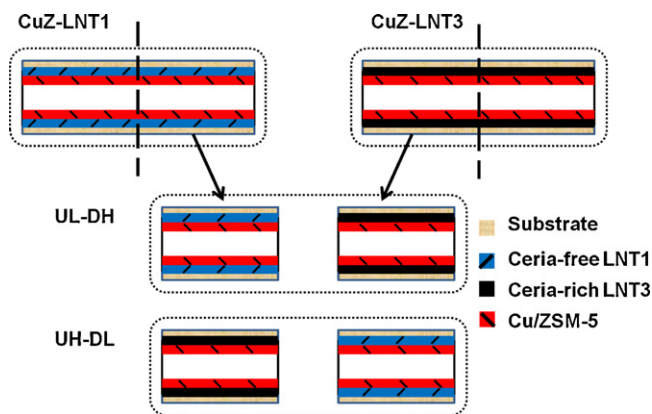
Fig. 9. Schematics of UL-DH and UH-DL zoned dual layer catalysts.

by the adjacent LNT layer. This consumes stored NH_3 that otherwise would react with NO_x [49]. At high temperatures, NH_3 oxidation generates NO_x. This downstream NH_3 oxidation decreases the high-temperature NO_x conversion below that of LNT3.

Non-uniform addition of ceria along the LNT layer; i.e. zoning can be used to balance low- and high-temperature NO_x reduction. The non-uniform loading of an active catalytic component is a practical method to increase the catalyst performance [43]. Dual-layer catalysts with different ceria profiles in the LNT layer were prepared by attaching halves of dual layer catalysts with different ceria loadings as shown in Fig. 9. The dual-zoned dual-layer catalyst is named using the following abbreviations. U (D) stands for the upstream (downstream) half-piece, L low ceria loading (0 wt%; LNT1), and H high ceria loading (34 wt%; LNT3). The dual-layer catalyst with a ceria-free upstream half-piece and a ceria-rich downstream half-piece is named as UL-DH. The dual-layer catalyst with a reverse ceria profile is UH-DL. Schematics of UL-DH and UH-DL are shown in Fig. 9.
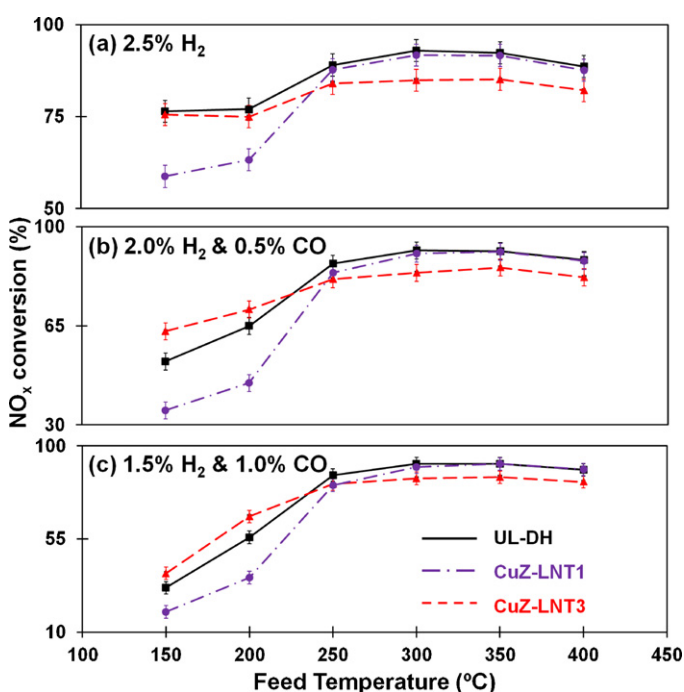

Fig. 10. The NO_x conversion by three dual-layer catalysts using mixtures with different 2.5% CO/H_2 reductant mixtures. The carrier gas contained 2.5% H_2O and 2.0% CO_2 in Ar.

Fig. 10a–c compares the NO_x conversion using different CO/H_2 reductant mixtures over three dual-layer catalysts: CuZ-LNT1 (ceria free), CuZ-LNT3 (ceria uniform – 34 wt.%), and UL-DH (no ceria in upstream, 34 wt.% in downstream). Using pure H_2 as the reductant (Fig. 10a), the CuZ-LNT3 low-temperature NO_x conversion exceeded by 18% that obtained by the ceria-free CuZ-LNT1 dual-layer catalyst. At higher temperatures, the NO_x conversion of the ceria-rich CuZ-LNT3 was lower by about 6% than that of the ceria-free CuZ-LNT1. The NO_x conversion of the dual-layer catalyst with a ceria-free front zone and a ceria-rich back zone (UL-DH) was higher than either the CuZ-LNT1 or the CuZ-LNT3 over the entire temperature range using H_2 as the sole reductant. When CO was included in the reductant mixture (Fig. 10b and c), the zoned dual-layer catalyst with an increasing ceria profile, UL-DH, still provided a good combination of the low- and high-temperatures merits of the CuZ-LNT1 and CuZ-LNT3, respectively. As Figs. 10b and c show, the NO_x conversion of UL-DH always exceeded that of CuZ-LNT1. The UL-DH had a higher NO_x conversion than CuZ-LNT3 above 250 °C, but a lower NO_x conversion below 250 °C. The ceria loading in UL-DH was only 50% of that in the CuZ-LNT3. Yet the NO_x conversion from the UL-DH was at most 10% lower than that of the CuZ-LNT3.

The non-uniform ceria loading of UL-DH enhances the NO_x conversion. Below 250 °C, the NO_x feed is mainly reduced by the downstream zone containing the high ceria loading. During the NO_x storage, ceria enhances the PGM activity for NO oxidation and NO_x spillover [15,30,40,44] and provides additional NO_x storage sites [11,30,40]; during the regeneration, ceria facilitates the reverse NO_x spillover to the PGM [15,30,40,44] and mitigates the CO inhibition [4,16]. The ceria-free upstream zone acts as a secondary NO_x reducer and an effective NH_3 generator at low temperatures [11]. On the other hand, above 250 °C, the majority of the fed NO_x is captured by the upstream ceria-free zone due to the enhanced LNT reactivity with temperature [11]. During the regeneration, the stored NO_x on the ceria-free upstream zone is reduced to NH_3 and the formed NH_3 is captured by the SCR top-layer. In the absence of ceria, the undesired NH_3 oxidation is lower than with ceria. Some escaping NH_3 is captured by the SCR top-layer in the downstream zone, instead of being oxidized by the LNT3 bottom-layer. Thus, the ceria-rich downstream zone can remove the slipping NO_x and NH_3 from the upstream zone. The synergy between the ceria-free upstream and the ceria-rich downstream zones enhances the loaded ceria utilization. Hence, the UL-DH is the best choice for NO_x reduction at both the low- and high-temperatures. Figs. 11a–c compare the NO_x conversions as a function of feed temperature from three dual-layer catalysts with different CO/H_2 reductant feed mixtures using three dual-layer catalysts with the same total ceria loadings (17 wt.%). In the CuZ-LNT2 the bottom layer was LNT2, which is uniformly loaded with ceria. The UL-DH always had a higher NO_x conversion than the other two catalysts over the entire temperature range for all the reductant mixtures. The performance of UH-DL was comparable to that of the CuZ-LNT2: The UH-DL low-temperature NO_x conversion was slightly higher than that of the CuZ-LNT2, which had a better high-temperature conversion.

The enhanced performance of UL-DH is due in part to a more effective utilization of the H_2 reductant. Ideally, an LNT should convert half the NO_x to NH_3 so that the emitted 1:1 NH_3:NO_x is converted to N_2 by selective catalytic reduction. However, in the presence of ceria, some H_2 reacts with adsorbed oxygen on Pt and on the ceria. Undesired hydrogen oxidation by an upstream ceria-rich catalyst decreases the NH_3 formation. A UL-DH zoning guarantees a maximum NH_3 formation in the ceria-free upstream zone. The remaining H_2 and CO reduce the stored NO_x on the ceria-rich downstream zone. Thus, a complete regeneration and a maximum NH_3 formation is obtained by the downstream ceria deposition. This also maximizes the contribution of the SCR top-layer to the NO_x reduction. The ceria-rich downstream zone serves
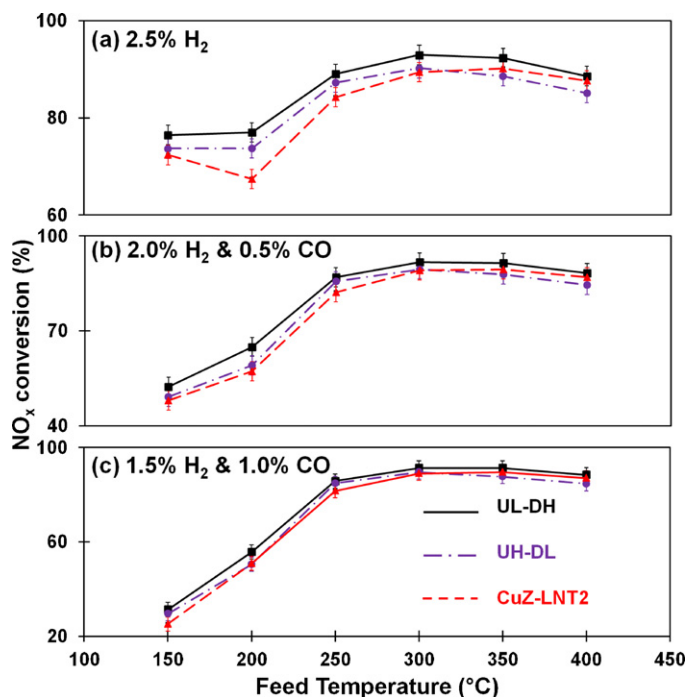
Fig. 11. Comparison of NO_x conversion by three different zoned dual-layer catalysts using 2.5% CO/H_2 reductant mixtures. The carrier gas contained 2.5% H_2O and 2.0% CO_2 in Ar.

Fig. 12. (a) The NO_x conversion and (b) NH_3 selectivity of an aged LNT1 catalyst with different 2.5% CO/H_2 reductant mixtures. The carrier gas contained 2.5% H_2O and 2.0% CO_2 in Ar.

as a major NO_x reducer at low temperatures and an NH_3 eliminator at high temperatures. The ceria-free upstream zone is the main NO_x reducer at high temperatures and the LNT bottom-layer generates NH_3 at all temperatures.

3.4. Using dual-layer catalyst to reduce PGM loading

A dual-layer catalyst can reduce NO_x by either the NSR or the SCR routes. It is desirable to replace some of the expensive LNT catalyst with the less expensive SCR catalyst. Thus, the PGM loading of the LNT catalyst should be the minimal needed to accomplish the partial storage and NH_3 generation. The LNT catalysts we used were not optimized for use in a LNT/SCR application. The high LNT washcoat loading probably caused diffusion limitations to exist especially at high temperatures. A lower loading of the LNT is likely to enable attaining the desired partial NO_x conversion and higher NH_3 selectivity. This is the subject of our current research.

Both hydrothermally aged and low PGM-loaded LNT catalyst have a low NO oxidation activity, and thus suffer from a low NO_x storage capacity. Both benefit from a high NH_3 selectivity due to the reduced NH_3 oxidation activity. Clayton et al. [34] showed that LNT catalysts having a low Pt dispersion are more effective NH_3 generation catalysts. Crocker and coworkers [44] have shown that aged LNT catalysts are more active NH_3 generation catalysts. Modeling has shown that the reduced activity is a consequence of the reduced rate of NO_x spillover from the barium to the PGM due to the less intimate contact between the PGM and the barium [34,47,50]. Thus, the local H_2/NO_x ratio over PGM increases during the regeneration, increasing the NH_3 selectivity.

Fig. 12a and b shows that the NO_x conversion and NH_3 selectivity of aged LNT1 are qualitatively similar to those of the fresh LNT1, as shown in Figs. 1 and 3. However, the NO_x conversion of the aged catalyst was lower by up to 30% from that of the fresh LNT1 catalyst, while the NH_3 selectivity was higher by approximately 10%. Hence, an aged LNT leads to a lower NO_x conversion and higher NH_3
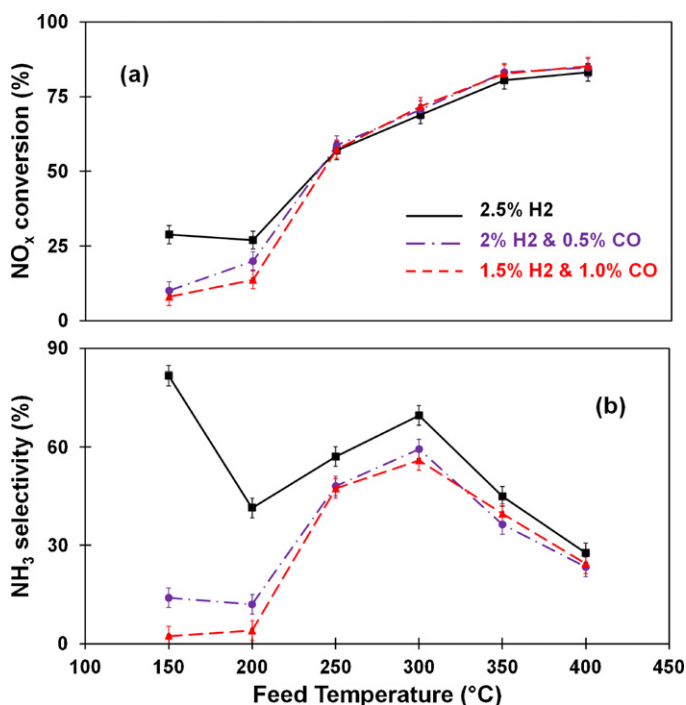
selectivity. To compensate for the declining activity of the aged LNT catalysts, a higher SCR loading (2.0 g/in^3) was applied to the dual-layer catalyst, i.e., instead of 0.9 g/in^3 in earlier experiments. Fig. 13 compares the cycle-averaged NO_x conversions using different reductant mixtures over three UL-DH catalysts: the first with a 0.9 g/in^3 SCR loading and a fresh LNT1 in the upstream followed by a
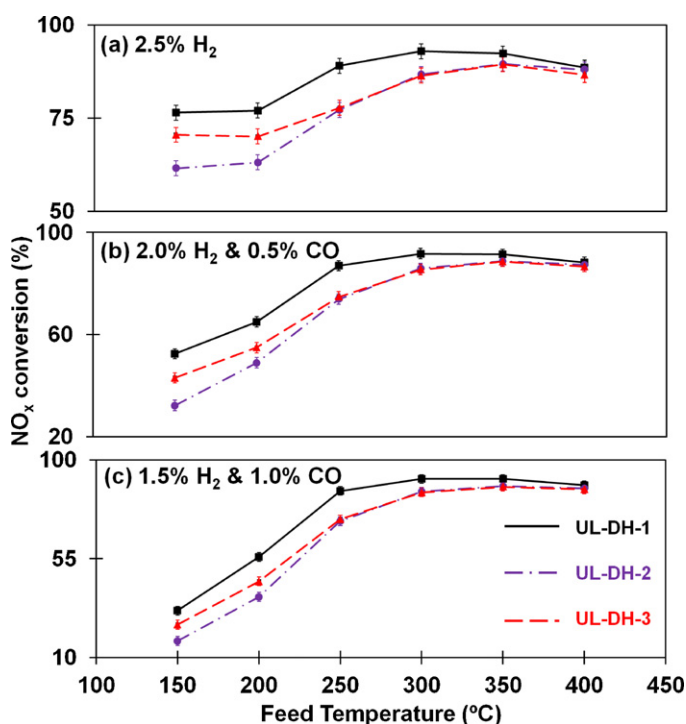

Fig. 13. The NO_x conversion by three zoned aged dual-layer catalysts with different SCR loadings using 2.5% CO/H_2 reductants mixtures. The carrier gas contained 2.5% H_2O and 2.0% CO_2 in Ar.

fresh LNT3 in the back (UL-DH-1; this is the UL-DH – the "1" distinguishes it from the other two catalysts); the second with a 0.9 g/in^3 SCR loading and an aged LNT1 in the upstream followed by a fresh LNT3 in the downstream (UL-DH-2); the third with a 2.0 g/in^3 SCR loading and an aged LNT1 in the upstream followed by a fresh LNT3 in the downstream (UL-DH-3). The UL-DH-1 dual-layer catalyst had the best performance for all reductant mixtures. The UL-DH-2 had the lowest NO$_x$ conversion in all cases. For the same LNT bottom-layer, the low-temperature NO$_x$ conversion could be increased by 8–10% by increasing the SCR loading. The impact of the SCR thickness decreased as the temperature is increased, The two dual-layer catalysts (UL-DH -2 and -3) with the aged LNT bottom-layer led to almost the same NO$_x$ conversion above 250 °C.

The experiments show that a thicker (higher loading) SCR layer can improve the low temperature NO$_x$ reduction performance, while the high temperature performance is comparatively less affected. This suggests that the low-temperature, dual-layer catalyst performance is limited by the SCR catalyst NH$_3$ utilization, while the high-temperature performance is limited by the NH$_3$ formation by the LNT catalyst. At low temperatures, the overall NO$_x$ reduction can be enhanced by using the LNT to convert the NO$_x$ to NH$_3$, and then using the SCR catalyst to react this NH$_3$ with NO$_x$. Since the standard SCR reaction (NO + O$_2$ + NH$_3$) over Cu/ZSM-5 is in the kinetic controlled regime below ca. 250 °C [11], notwithstanding the fact that the SCR catalyst in the current study has a lower activity, a higher SCR loading increases the NO$_x$ conversion. Upon a temperature increase to 300 °C, NO$_x$ reduction by the SCR top-layer is limited by the NH$_3$ generated by the LNT bottom-layer and not by the SCR catalytic activity. Increasing the SCR loading cannot improve the high-temperature NO$_x$ conversion. In this scenario, the NO$_x$ reduction is limited by the NO$_x$ storage and sequential NH$_3$ generation on the LNT catalyst. The SCR contribution is limited by the rate of NH$_3$ formation by the LNT bottom-layer. A Moreover, too high of a SCR layer loading may cause diffusion limitations that would decrease the reactor productivity. This is another current research of our group.

The low-temperature NO$_x$ reduction by a dual-layer catalyst with aged LNT bottom-layer can be improved by increasing the SCR loading. The dual-layer catalyst offers an opportunity to reduce the PGM loading by enhancing the SCR reactions at low temperatures. In the operating temperature window of 150–400 °C, the rate of NO$_x$ reduction on the LNT is limited at low temperatures, due to kinetic limitations of NO oxidation and NO$_x$ regeneration. Thus, a high PGM loading is needed to achieve a desired low temperature NO$_x$ conversion. Some of this PGM is not needed at high temperatures. Increasing the SCR loading enables a lowering of the PGM load to a level that provides the required NO$_x$ conversion at both low and high temperatures.

The dual-layer catalyst provides an effective and practical solution to reduce PGM loading at high temperatures. One can estimate the efficiency of the loaded PGM by a space time yield defined as followed:

$$STY_{PGM} \left(\frac{\text{mol NO}_x \text{ converted}}{\text{g PGM h}} \right) = \frac{X_{NO_x} F_{NO_x}^o (\text{mol NO}x \text{ fed/h})}{\text{PGM loading (g)}} \quad (4)$$

A high value of STY$_{PGM}$ corresponds to a low loading of PGM needed to achieve a specified NO$_x$ conversion rate. Table 2 compares the STY$_{PGM}$ of different LNT/SCR combinations from different groups at 300 °C. The dual-layer catalyst has the highest STY$_{PGM}$ value. Since the precious group metals, such as Pt and Rh are the most expensive components in the LNT/SCR, a dual-layer catalyst can reduce the catalyst cost. The successful application of the aged LNT in the dual-layer LNT/SCR catalyst suggests possible use of a LNT catalyst containing a smaller PGM loading. Research on further reduction

Table 2
STY$_{PGM}$ at 300 °C of several LNT-SCR catalysts configurations.

Source	Catalyst configuration	STY$_{PGM}$ (mol/h gPGM)
This paper	Dual-layer	0.38
Ref. [48]	Multi-brick	0.17
Ref. [9]	Dual-bed	0.18
Ref. [29]	Mixture	0.30

of STY$_{PGM}$ with low PGM-loaded dual-layer catalyst is ongoing.

3.5. Optimization of lean-rich cycle time

Kabin et al. [45] studied the dependence of the time-averaged NO$_x$ conversion and N$_2$ selectivity on the lean-rich protocol. Clayton et al. [46] and Ren et al. [15] extended that work. The rich time needs to be sufficiently long to avoid dilution of the rich feed and to generate NH$_3$. Too long of a rich time causes excessive breakthrough of reductant. Thus, an optimal intermediate cycle duration exists. At a fixed lean time and feed composition, the NH$_3$ selectivity increases with the rich time. Due to the important role of NH$_3$ in the protocol for the dual-layer catalyst, its optimal lean-rich cycle time differs from that used for the LNT-only catalyst.

Fig. 14a and b respectively describe the NO$_x$ and H$_2$ conversions under different rich pulse durations using the UL-DH-3 dual-zoned aged dual-layer catalyst. The lean phase feed was fixed at 500 ppm NO and 5% O$_2$ in a carrier gas mixture containing 2.5% H$_2$O and 2.0% CO$_2$ in Ar. The lean duration was 60 s while the rich cycle duration varied from 3 to 20 s. The total amount of H$_2$ fed during the rich period was 93.0 μmol, achieved by adjusting the H$_2$ feed concentration for the different durations. The 60-3 lean-rich cycle had the lowest NO$_x$ conversion over the entire temperature range (Fig. 14a). The NO$_x$ conversion was most sensitive to the rich pulse intensity at low temperatures (<250 °C). In contrast, at high temperatures (>300 °C) the sensitivity NO$_x$ conversion to the rich pulse intensity was confined to a smaller range of NO$_x$ conversions.
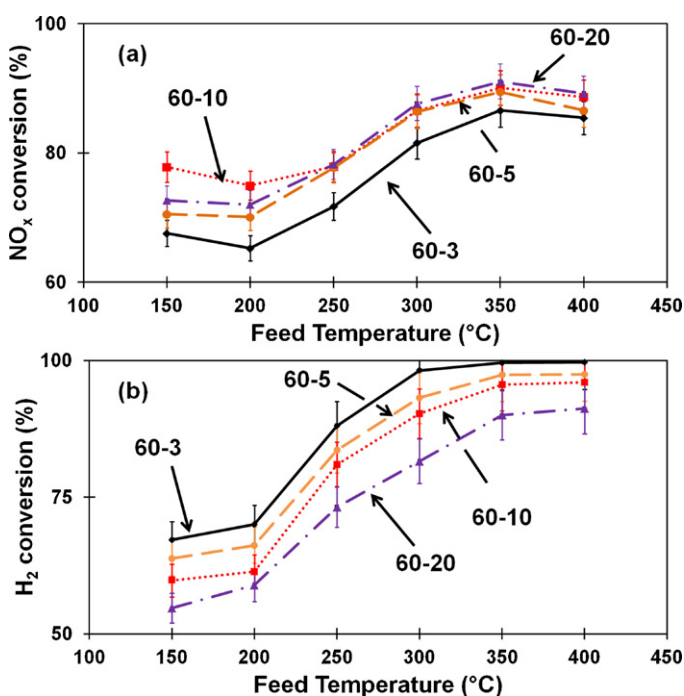

Fig. 14. Impact of lean-rich cycle ratios on (a) NO$_x$ and (b) H$_2$ conversion by a zoned aged UL-DH-3 dual-layer catalyst.
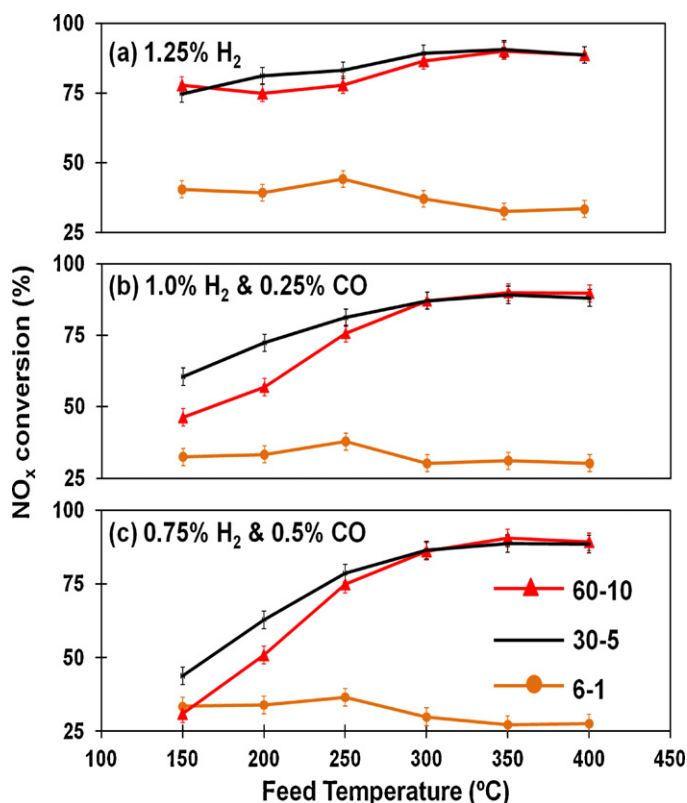
Fig. 15. Comparison of NO_x conversion under different lean-rich cycles by an aged zoned UL-DH-3 catalyst using mixtures with 1.25% CO/H_2 reductants mixtures. The carrier gas contained 2.5% H_2O and 2.0% CO_2 in Ar.

At low temperature (<250 °C) the 60s lean/10s rich gave the highest conversion while above this temperature the 60s lean/20s rich was best. For example, at 200 °C the NO_x conversion from the 60-5 lean-rich cycles exceeded that of the 60-3 cycle but was smaller than that of the 60-10 cycle. An increase in the rich duration to 20s and corresponding decrease in the H_2 concentration decreased the NO_x conversion below that of the 60-10 lean-rich cycle.

The peak NO_x conversion at the 60-10 lean-rich cycle obtained at low temperature may be due to the maximum H_2 efficiency for NH_3 formation. According to an IR thermography study by Liu et al. [16], the reductant reacts with the residual oxygen held in the catalyst pores upon the switch from lean to rich phase. For a short rich duration with high H_2 concentration, a non-negligible fraction of the H_2 is wasted in the very beginning by reaction with residual O_2. This decreases the amount of H_2 available for stored NO_x regeneration and increases the H_2 conversion. The NH_3 produced during the rich phase decreases as well. A longer duration rich phase feed with a lower H_2 concentration minimizes the undesired hydrogen oxidation and decreases the H_2 consumption. On the other hand, too low of a H_2 concentration decreases the H_2/NO_x ratio, favoring the N_2 formation instead of NH_3, decreasing the NO_x reduction by the SCR layer. This is undesirable if the goal is to increase the NO_x reduction by the SCR catalyst. Hence, an optimal rich duration and H_2 concentration exist for maximum H_2 efficiency and NH_3 production. For instance, in our study the optimal rich duration and H_2 concentration are 10 s and 1.25%, respectively.

Optimization of the lean-rich cycle increases the fuel economy. For example, a processing time of 910s corresponds to thirteen 60-10 cycles and fourteen 60-5 cycles. The total amount of H_2 injected is 1209 μmol for the 60-10 lean-rich cycle and 1302 μmol for the 60-5 lean-rich cycle. Since the 60-10 lean-rich cycle reduces the

amount of H_2 injection, the amount of reductant needed for catalyst regeneration is minimized. The fuel economy can be further improved by shortening the rich duration to avoid excessive H_2 breakthrough and increase the H_2 conversion.

Additional optimization was done for a fixed 6:1 ratio of lean to rich duration, while the total cycle time was varied from 7 to 70 s. Experiments were conducted with three lean-rich cycles: 6s-1a, 30s-5s and 60s-10s. Fig. 15 shows the NO_x conversion from these three lean-rich cycles with different reductants. The 6s-1s lean-rich cycle had the lowest NO_x conversion under all conditions, and the feed temperature had little impact on the NO_x conversion. The advantage of 30s-5s lean-rich cycle over the 60s-10s lean-rich cycle was significant when the temperature was below 300 °C, while these two cycles led to similar NO_x conversion above 300 °C.

A high lean-rich cycling frequency increases the utilization of the available NO_x storage sites. Shakya et al. [47] used a crystallite-scale LNT model to simulate different lean-rich cycles over a low-dispersion LNT catalyst. A short lean-rich cycle improves the $deNO_x$ performance, when the storage and reduction are limited by the transport of stored NO_x. More effective NO_x storage and NH_3 generation in the LNT layer enhances the $deNO_x$ performance of the dual-layer catalyst. Hence, the NO_x conversion by the UL-DH-3 dual-zoned dual-layer catalyst can be improved by a short lean-rich cycle. One important benefit from the short lean-rich cycle is the increase of NO_x conversion in the presence of CO at low temperatures. This implies the possibility to increase the air-to-fuel ratio during the catalyst regeneration, enhancing the fuel economy. On the other hand, a too short lean-rich cycle is harmful to the catalyst performance. According to the reports from Kabin et al. [45], the short rich duration dilutes the rich feed so that a reducing environment cannot be created. As a result, the 6s-1s lean-rich cycle has the lowest NO_x conversion among all the three tested lean-rich cycles.

4. Concluding remarks

The experiments with LNT-SCR dual-layer catalysts reveal that it is an attractive design alternative that adjustments of the catalyst design and operating strategies may enhance NO_x reduction, lower the PGM loading and increase the fuel economy. The main findings are:

- CO inhibition of the LNT catalyst at low temperatures is a key obstacle for NO_x reduction when using mixtures of H_2 and CO. Increasing the SCR loading on the dual-layer catalyst improves the low-temperature NO_x reduction.
- Ceria addition to the LNT layer improves the low-temperature NO_x reduction by enhancing the reverse water-gas-shift reaction, but an undesirable impact is the enhancement of NH_3 oxidation at high temperatures.
- Zoned ceria deposition of the LNT catalyst may improve the low temperature NO_x reduction and minimizes NH_3 oxidation at high temperatures. For a fixed total ceria loading, the NO_x conversion by a dual-layer catalyst with a ceria-free upstream zone and a ceria-rich downstream zone is 5–10% higher than one with a uniform ceria profile.
- The PGM loading of a dual-layer catalyst may be reduced by increasing the SCR loading. A high SCR loading improves the low-temperature NO_x conversion, while the NO_x conversion above 250 °C is limited by NO_x storage and the subsequent NH_3 formation from the LNT catalyst.
- Adjustment of the ratio of lean to rich feed time and the total duration of lean-rich cycle can increase the NO_x conversion and enable minimizing the impact of CO inhibition at low temperatures.

Acknowledgements

References

[1] John Chi, Herbert DaCosta, SAE 2005-01-0966.
[2] John Chi, SAE 2009-01-0905.
[3] K. Kamasamudram, A. Yezerets, X. Chen, N. Currier, M. Castagnola, H. Chen. SAE 2011-01-1314.
[4] W. Epling, L. Campbell, A. Yezerets, N. Currier, J. Parks II, Catalysis Reviews 46 (2004) 163–245.
[5] Z. Liu, S. Woo, Catalysis Reviews 48 (2006) 43–89.
[6] A. Lindholm, H. Sjövall, L. Olsson, Applied Catalysis B: Environmental 98 (2010) 112–121.
[7] B. Pereda-Ayo, D. Duraiswami, J.R. González-Velasco, Catalysis Today 172 (2011) 66–72.
[8] R. Bonzi, L. Lietti, L. Castoldi, P. Forzatti, Catalysis Today 151 (2010) 376–385.
[9] P. Forzatti, L. Lietti, Catalysis Today 155 (2010) 131–139.
[10] L. Castoldi, R. Bonzi, L. Lietti, P. Forzatti, S. Morandi, G. Ghiotti, S. Dzwigaj, Journal of Catalysis 282 (2011) 128–144.
[11] Y. Liu, M.P. Harold, D. Luss, Applied Catalysis B: Environmental 121–122 (2012) 239–251.
[12] J.H. Kwak, D.H. Kim, J. Szanyi, C.H.F. Peden, Applied Catalysis B: Environmental 84 (2008) 545–551.
[13] L. Lietti, I. Nova, P. Forzatti, Journal of Catalysis 257 (2008) 270–282.
[14] F. Frola, F. Prinetto, G. Ghiotti, L. Castoldi, I. Nova, L. Lietti, P. Forzatti, Catalysis Today 126 (2007) 81–89.
[15] Y.J. Ren, M.P. Harold, ACS Catalysis 1 (2011) 969–988.
[16] Y. Liu, M.P. Harold, D. Luss, Applied Catalysis A-General 397 (2011) 35–45.
[17] D.S. Lafayatis, G.P. Ansell, S.C. Bennett, J.C. Forst, P.J. Millington, R.R. Rajaram, A.P. Walker, T.H. Ballinger, Applied Catalysis B: Environmental 18 (1998) 123–135.
[18] P. Forzatti, L. Lietti, I. Nova, S. Morandi, F. Prinetto, G. Ghiotti, Journal of Catalysis 274 (2010) 163–175.
[19] L. Castoldi, L. Lietti, R. Bonzi, N. Artioli, P. Forzatti, S. Morandi, G. Ghiotti, Journal of Physical Chemistry C 115 (2011) 1277–1286.
[20] C.D. DiGiulio, V.G. Komvokis, M.D. Amiridis, Catalysis Today 184 (2012) 8–19.
[21] J. Theis, H.-W. Jen, R. McCabe, M. Sharma, V. Balakotaiah, M.P. Harold. SAE 2006-01-1067.
[22] T. Szailer, J.H. Kwak, D.H. Kim, J.C. Hanson, C.H.F. Peden, J. Szanyi, Journal of Catalysis 239 (2006) 51–64.
[23] D. James, E. Fourre, M. Ishii, M. Bowker, Applied Catalysis B: Environmental 45 (2003) 147–159.
[24] S. Poulston, R.R. Rajaram, Catalysis Today 81 (2003) 603–610.
[25] Y. Li, S. Roth, J. Dettling, T. Beutel, Topics in Catalysis 16/17 (2001) 139–144.
[26] C.M.L. Scholz, B.H.W. Maes, M.H.J.M. de Croon, J.C. Schouten, Applied Catalysis A-General 332 (2007) 1–7.
[27] P. Jozsa, E. Jobson, M. Larsson, Topics in Catalysis 30/31 (2004) 177–180.
[28] P.R. Dasari, R. Muncrief, M.P. Harold, Catalysis Today 184 (2012) 43–53.
[29] E.C. Corbos, M. Haneda, X. Courtois, P. Marecot, D. Duprez, H. Hamada, Applied Catalysis A-General 365 (2009) 187–193.
[30] J. Wang, Y. Ji, Z. He, M. Crocker, M. Dearth, R.W. McCabe, Applied Catalysis B: Environmental 111–112 (2012) 562–570.
[31] P.S. Metkar, N. Salazar, R. Muncrief, V. Balakotaiah, M.P. Harold, Applied Catalysis B: Environmental 104 (2011) 110–126.
[32] K.S. Kabin, P. Khanna, R.L. Muncrief, V. Medhekar, M.P. Harold, Catalysis Today 114 (2006) 72–85.
[33] R.D. Clayton, M.P. Harold, V. Balakotaiah, Applied Catalysis B: Environmental 84 (2008) 616–630.
[34] R.D. Clayton, M.P. Harold, V. Balakotaiah, C.Z. Wan, Applied Catalysis B: Environmental 90 (2009) 662–676.
[35] Y. Liu, Y. Zheng, M.P. Harold, D. Luss, Topics in Catalysis, in press.
[36] E.C. Corbos, M. Haneda, X. Courtois, P. Marecot, D. Duprez, H. Hamada, Catalysis Communications 10 (2008) 137–141.
[37] T. Morita, N. Suzuki, N. Satoh, K. Wada, H. Ohno, SAE 2007-01-0239.
[38] K. Wada, N. Suzuki, N. Satoh, T. Morita, S. Yamaguchi, H. Ohno, SAE 2007-01-1933.
[39] A.A. Phatak, N. Koryabkina, S. Rai, J.L. Ratts, W. Ruettinger, R.J. Farrauto, G.E. Blau, W.N. Delgass, F.H. Ribeiro, Catalysis Today 123 (2007) 224–234.
[40] Y. Ji, J.S. Choi, T.J. Toops, M. Crocker, M. Naseri, Catalysis Today 136 (2008) 146–155.
[41] M.P. Harold, M.E. Garske, Journal of Catalysis 127 (1991) 524–552.
[42] M.P. Harold, M.E. Garske, Journal of Catalysis 127 (1991) 553–575.
[43] J. Ura, J. Theis, C. Goralski, US Patent 7870724.
[44] Y. Ji, V. Easterling, U. Graham, C. Fisk, M. Crocker, J.S. Choi, Applied Catalysis B: Environmental 103 (2011) 413–427.
[45] Kabin, K.R.L. Muncrief, M.P. Harold, Y. Li, Chemical Engineering Science 59 (2004) 5319–5532.
[46] R.D. Clayton, M.P. Harold, V. Balakotaiah, AIChE Journal 55 (2009) 687–700.
[47] B. Shakya, M.P. Harold, V. Balakotaiah, Catalysis Today 184 (2012) 27–42.
[48] J. Theis, M. Dearth, R. McCabe, SAE 2011-01-0305.
[49] R.D. Clayton, M.P. Harold, V. Balakotaiah, Applied Catalysis B: Environmental 81 (2008) 161–181.
[50] D. Bhatia, R.D. Clayton, V. Balakotaiah, M.P. Harold, Catalysis Today 151 (2010) 314–329.